



Cortical atrophic-hypometabolic dissociation in the transition from premanifest to early-stage Huntington's disease

Frederic Sampedro^{1,2,3} · Saul Martínez-Horta^{1,2,3,4} · Jesús Perez-Perez^{1,2,3,4,5} · Andrea Horta-Barba^{1,2,4} · Diego Alfonso Lopez-Mora⁶ · Valle Camacho⁶ · Alejandro Fernández-León⁶ · Beatriz Gomez-Anson^{5,7} · Ignasi Carrió^{5,6} · Jaime Kulisevsky^{1,2,3,4,5}

Received: 24 October 2018 / Accepted: 27 December 2018 / Published online: 9 January 2019
© Springer-Verlag GmbH Germany, part of Springer Nature 2019

Abstract

Purpose Huntington's disease (HD) is a fatal neurodegenerative disorder with no effective treatment currently available. Although the pathological hallmark of HD is massive striatal atrophy, it has been suggested that cortical deterioration may concomitantly occur and play a major role in the patient's functional independence. Our objective was to characterize cortical structural and metabolic neurodegeneration in the transition from premanifest to early-stage Huntington's disease (HD).

Methods Using a surface-based neuroimaging approach, we compared cortical thickness and intracortical FDG-PET uptake in 19 early-symptomatic HD patients with respect to 21 premanifest HD individuals.

Results Early-HD patients showed significant cortical atrophy and intracortical hypometabolism when compared to premanifest subjects ($p < 0.05$, corrected for multiple comparisons). However, whereas the atrophy pattern was restricted to precentral and parieto-occipital regions, a pronounced frontotemporal hypometabolism was observed. Importantly, structural changes correlated with motor and cognitive performance, and metabolic changes were associated with the presence and severity of apathy in this population, a core neuropsychiatric feature of this disorder.

Conclusion Our findings reveal an asynchronous neuronal loss and metabolic compromise across the cerebral cortex in early HD. Hence, the use of structural and metabolic imaging indicators to characterize disease progression in this population should take into consideration the dissociation which occurs between cortical atrophy and hypometabolism.

Keywords Huntington's disease · ¹⁸F-FDG-PET · Cortical thickness · Partial volume correction

Introduction

Huntington's disease (HD) is a fatal neurodegenerative disorder driven by an abnormal CAG expansion of the *HTT* gene.

With no effective treatment currently available, progressive motor, cognitive, and neuropsychiatric alterations result in a devastating clinical outcome of HD patients. Even though the pathological hallmark of HD is a massive loss of the medium spiny neurons of the striatum, cortical deterioration concomitantly occurs and also contributes to a severe compromise of the individual's functional independence [1, 2].

Using magnetic resonance imaging (MRI), progressive structural brain deterioration along the disease continuum has been well-documented, and is known to be detectable up to 15 years before symptoms appear [3, 4]. In HD, novel therapeutic approaches are being developed aiming to stop or delay the neurodegenerative process. In this context, *in vivo* imaging biomarkers are of special interest to potentially be used to monitor therapy outcomes.

Given that reversing brain atrophy is presently unattainable with current treatment strategies, understanding the functional brain abnormalities occurring in early stages of HD could reveal new therapeutic targets. It should be noted that

✉ Jaime Kulisevsky
jkulisevsky@santpau.cat

¹ Movement Disorders Unit, Neurology Department, Hospital de la Santa Creu i Sant Pau, Mas Casanovas 90, 08041 Barcelona, Spain

² Biomedical Research Institute (IIB-Sant Pau), Barcelona, Spain

³ Centro de Investigación en Red-Enfermedades Neurodegenerativas (CIBERNED), Barcelona, Spain

⁴ European Huntington's Disease Network (EHDN), Ulm, Germany

⁵ Autonomous University of Barcelona, Barcelona, Spain

⁶ Nuclear Medicine Department, Hospital de la Santa Creu i Sant Pau, Barcelona, Spain

⁷ Neuroradiology, Radiology Department, Hospital de la Santa Creu i Sant Pau, Barcelona, Spain

promising results have been reported with regard to drug-induced increases in brain metabolism, which could prevent or delay a subsequent neuronal loss [5–7].

However, studies of metabolic changes in HD using 18F-FDG-PET/CT scans are scarce and have important limitations [8]. On one hand, heterogeneous samples with reduced number of patients prevent an accurate metabolic characterization of premanifest and early-stage HD. On the other hand, appropriate partial volume correction (PVC) techniques using co-registered T1-MRI scans have not been applied in most studies, thereby making it difficult to evaluate whether the observed metabolic deficits were merely a consequence of already-existing brain atrophy. This latter issue is particularly relevant, as it has recently been shown that different PVC methods might lead to different imaging conclusions [9].

Furthermore, studies concerning surface-based analysis of intracortical FDG-PET uptake in HD are currently lacking. As shown by Greve et al. in their seminal paper [10], the use of a surface-based approach in this context provides substantial improvements in reliability and detectability of metabolic effects in the cerebral cortex. Hence, its application in premanifest and early-stage HD cases, which are typically limited in terms of size due to the relatively low prevalence of the disease, appears especially indicated.

In this work, we characterize cortical neurodegeneration in the transition from premanifest to early-stage HD by means of a surface-based analysis of FDG-PET uptake and cortical thickness.

Materials and methods

Participants and clinical assessments

We included 40 gene mutation carriers ($CAG \geq 39$) from the outpatient clinic of the Movement Disorders Unit at the Hospital de la Santa Creu i Sant Pau (Barcelona, Spain). Participants were classified as premanifest HD (preHD) and early-symptomatic HD (earlyHD). Individuals with a Unified Huntington's Disease Rating Scale (UHDRS) total motor score (TMS) below 5 and a diagnostic confidence level (DCL) < 3 were classified as preHD. Patients showing a total motor score ≥ 5 , a DCL of 4, and a TFC score between 11 and 13 were classified as earlyHD [11].

Clinical data regarding the hallmark symptoms of HD were also recorded. UHDRS-TMS scores were used to characterize motor symptoms, and cognitive measures were obtained using the UHDRS cognitive score (Cogscore). The severity of neuropsychiatric symptoms was addressed with the apathy score derived from the Problem Behaviors Assessment for HD (PBA-s) [12], as apathy is probably the most representative symptom of this type in HD [13]. Finally, TFC scores were also considered to model the overall patient's functionality.

Neuroimaging acquisition and methods

All participants had available structural magnetic resonance imaging (MRI) and 18F-FDG-PET scans. T1-weighted MRI scans were acquired in a 3 T Philips Achieva, and were performed using a dedicated axial T13D-magnetization-prepared rapid gradient-echo (T13D-MP-RAGE) MRI: Repetition time/Echo time (TR/TE) 500/50 milliseconds, flip-angle = 8° , field of view (FOV) = 23 cm, an in-plane resolution of 256×256 and 1-mm slice thickness. ^{18}F -FDG PET/CT scans were acquired on a Philips Gemini TF station 60 min after the intravenous injection of 277 MBq/ml of radiotracer, and following the European Association of Nuclear Medicine procedural guidelines for PET brain imaging [14].

Cortical thickness (Cth) analysis was performed using the FreeSurfer 6.0 software package (<https://surfer.nmr.mgh.harvard.edu/>). The specific methods employed for cortical reconstruction of structural T1-MRI images have been fully described elsewhere [15]. Briefly, optimized surface deformation models following intensity gradients are able to accurately identify white matter and gray matter boundaries in the cerebral cortex, from which cortical thickness is computed at each vertex. On visual inspection, no major surface reconstruction errors were observed in our sample.

Intracortical ^{18}F -FDG PET uptake was studied through the PetSurfer pipeline [9, 10] (<https://surfer.nmr.mgh.harvard.edu/fswiki/PetSurfer>). In short, PET images were registered to its associated T1-MRI scans, intensity-scaled with respect to the pons region to obtain relative standardized uptake values (SUVr), partial-volume corrected using the Müller–Gartner method and sampled halfway between the white and pial surfaces. SUVr values are needed for the study of tracer uptake differences in cerebral PET scans to avoid the inclusion of undesired variations in absolute SUV values. By dividing each voxel's tracer uptake by the mean uptake within a reference region, the resulting SUVr values can be reliably compared across subjects. The choice of reference region is important, as its metabolism should be most stable within the group under study in order not to introduce intensity-normalization artifacts. As the pons metabolism has recently been shown to be highly preserved in manifest HD patients with respect to presymptomatic individuals [16], it was used as the reference region in our SUVr computation.

Although the main focus of this work was to study structural and metabolic cortical differences across HD groups, we also computed mean PVC-SUVr values and volumetric information in common subcortical structures.

Statistical analyses

Clinical and sociodemographic data were compared across groups using two-sample *t*-test analysis for continuous

variables and X^2 for categorical variables. Differences were considered significant using a probability value (p -val) < 0.05 .

Cortical vertexwise measures (Cth and SUVr) were first smoothed using a Gaussian kernel of 10 mm full-width-at-half-maximum (FWHM) to increase the signal-to-noise ratio. Then, a generalized linear model (GLM) was performed to compare preHD and earlyHD groups, using age, sex, and education as covariates of no interest. Clusters surviving $p < 0.05$ and family-wise error (FWE) correction for multiple comparison by a Monte-Carlo simulation with 10,000 repeats were considered significant. We also compared subcortical volumetric and SUVr information across HD groups using the same GLM.

Finally, mean Cth and SUVr values at the identified cortical clusters were computed and correlated with clinical indicators in an exploratory analysis using Pearson's correlation coefficients. An analogous analysis was performed with subcortical volumetric and SUVr information in those regions, showing significant differences across groups. A p -val < 0.05 was considered significant.

For the statistical vertexwise imaging analyses, the `mri_glmfit` and `mri_glmfit-sim` FreeSurfer tools were used. Statistic analysis concerning clinical and sociodemographic comparisons as well as clinical-imaging associations was conducted with the SPSS v15 software package.

Results

Table 1 summarizes the sociodemographic and clinical data of the sample. As expected, early-HD patients were older. They also had lower education and presented with worse motor, cognitive and apathy scores.

Figure 1 shows the set of cortical atrophic and hypometabolic regions found in the earlyHD group when compared to preHD. Whereas cortical atrophy was mostly observed in precentral and parieto-occipital regions, a pronounced frontotemporal hypometabolism was revealed.

Mean Cth and FDG-SUVr values at the identified atrophic and hypometabolic clusters were computed and correlated with clinical indicators. We found the following significant associations: Considering the whole HD group, Cth values in all atrophic clusters inversely correlated with UHDRS-TMS scores and positively correlated with UHDRS-Cogscore measures (all showing $p < 0.005$ and r coefficients in the 0.47–0.76 range). Additionally, apathetic patients showed reduced FDG-SUVr values in all the observed hypometabolic clusters ($p < 0.05$ and r values ranging from 0.32 to 0.34).

Within the preHD group, stronger correlations were obtained between the presence of apathy and SUVr values at the hypometabolic clusters (all $p < 0.02$, and r between 0.49 and 0.59), and UHDRS-TMS scores correlated with Cth values at

two parietotemporal atrophic clusters ($p = 0.018$, $r = -0.51$; $p = 0.021$, $r = -0.50$). Finally, in the earlyHD group, the following atrophic clusters were related to clinical indicators: UHDRS-Cogscore and UHDRS-TMS scores with precentral and parieto-temporal regions (all $p < 0.03$, r from 0.47 to 0.64), and TFC measures with precentral and parieto-occipital regions (all $p < 0.04$, r from 0.46 to 0.69). Additionally, when controlling for CAG-length and UHDRS-TMS scores, a significant association between left frontal SUVr and apathy scores was also observed in this group ($r = -0.81$, $p = 0.026$).

With regard to structural or metabolic differences in subcortical structures across groups, Table 2 shows subcortical volumetric and SUVr values and their statistical significance.

Considering the whole HD group, both volumes and SUVr values at bilateral caudate and putamen regions inversely correlated with UHDRS-TMS scores and positively correlated with UHDRS-Cogscore measures (all $p \leq 0.001$ and r coefficients in the 0.51–0.77 range). Pallidum volumes (bilaterally) also inversely correlated with UHDRS-TMS scores and positively correlated with UHDRS-Cogscore measures ($p \leq 0.001$, r coefficients in the 0.52–0.74 range). Apathetic patients showed reduced SUVr values both at the caudate and putamen regions, but only decreased volume in the caudate region (all $p \leq 0.01$ and r coefficients in the 0.39–0.47 range).

Within the preHD group, UHDRS-TMS scores only correlated with bilateral caudate and left putamen volumes ($p \leq 0.02$ and r in the range 0.49–0.50). Apathetic patients only showed reduced SUVr values at bilateral putamen and left caudate ($p < 0.05$, r in the range 0.44–0.48). Left caudate volumes positively correlated with UHDRS-Cogscore measures ($p = 0.026$, $r = 0.48$). Finally, in the earlyHD group, left caudate SUVr values correlated with UHDRS-TMS scores ($p = 0.03$, $r = -0.49$) and apathetic patients only showed reduced left caudate volume ($p = 0.019$, $r = 0.5$). No subcortical imaging indicators correlated with TFC scores in any group.

Discussion

This is the first study to explore intracortical metabolic changes between premanifest and early-stage HD patients. Notably, concomitant but not overlapping cortical hypometabolic and atrophic patterns were found in earlyHD patients. On one hand, the presence of atrophy in precentral and parieto-occipital regions, whose integrity correlated with clinical motor and cognitive scores, is in line with previous works in this context [17, 18]. On the other hand, we observed a widespread frontotemporal hypometabolism that related to apathy severity, a core neuropsychiatric feature of HD that can be detected many years before motor onset [13].

As expected, striatal atrophy and hypometabolism were also found, which in turn also correlated with motor and

Table 1 Clinical and sociodemographic characteristics

	HD	Premanifest HD	Early-symptomatic HD	<i>P</i> value
<i>N</i>	40	21	19	
Age (years)	45.3 ± 14.2	37.7 ± 10.8	53.7 ± 12.8	< 0.001
Sex	30% male	24% male	36% male	0.37
Education (years)	13.2 ± 4.7	15.1 ± 3.6	11.1 ± 4.9	0.007
CAG length	42.6 ± 2.9	42.4 ± 3.2	42.7 ± 2.7	0.83
UHDRS-TMS	11.7 ± 14.4	1.33 ± 1.5	23.2 ± 13.5	< 0.001
TFC	12.6 ± 0.8	12.9 ± 0.2	12.1 ± 0.9	0.001
UHDRS-Cogscore	253.2 ± 82.4	309.7 ± 49.9	187.3 ± 60.8	< 0.001
Apathy score	3.5 ± 4.5 (47% apathetic)	2.1 ± 3.4 (33% apathetic)	5.2 ± 5.1 (63% apathetic)	0.03

Values are expressed as mean ± standard deviation

Apathy score was derived from the Problem Behaviors Assessment for HD (PBA-s), and patients with PBA-s > 2 were considered apathetic

CAG cytosine-adenine-guanine, UHDRS-TMS Unified Huntington's Disease Rating Scale-total motor score, TFC total functional capacity, UHDRS-Cogscore Unified Huntington's Disease Rating Scale-cognitive sScore

cognitive indicators. Interestingly, however, only precentral and posterior-cortical atrophy correlated with TFC scores, the most commonly used clinical outcome of functional independence in HD.

These findings reveal an asynchronous neural loss and metabolic compromise across the cerebral cortex, which contributes to an understanding of the timing of the neurodegeneration occurring in this disorder. Importantly, our results also highlight the important contribution of posterior-cortical degeneration to cognitive decline in HD. Although the contribution of the observed early fronto-temporal hypometabolism to HD cognition remains to be clarified, this observation further encourages the scientific and medical community to study cognitive changes in HD in the light of an underlying brain compromise that extends beyond fronto-striatal territories [19, 20].

Differential cortical atrophy and hypometabolic pattern in earlyHD

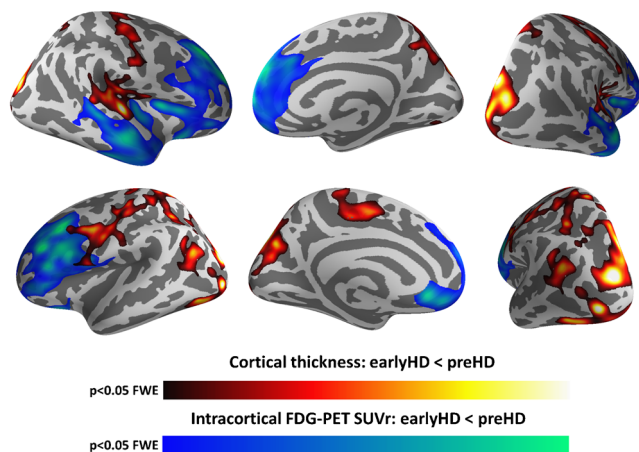


Fig. 1 Brain regions where earlyHD patients showed cortical thinning and reduced FDG-PET SUVR values with respect to preHD subjects, using age, sex, and education as covariates of no interest ($p < 0.05$, corrected for multiple comparisons)

It is noteworthy that the detection of frontotemporal hypometabolism in early-HD may prove key to better characterizing the physiopathological nature of common neuropsychiatric symptoms observed in this population. In particular, apathy seems to be one of such core HD features that reflect a metabolic cortico-subcortical compromise in the early stages of the disorder. Given its major impact on quality of life, boosting brain glucose metabolism may prove useful to ameliorate this behavioral symptom. In this respect, other common behavioral features seen in HD such as irritability or perseveration should also be considered in future research.

From an imaging perspective, the fact that the clinical onset of HD is evidence of a structural cortical damage without an associated metabolic compromise needs to be taken into consideration. This observation, which is probably due to a partial volume effect, implies that imaging indicators derived from FDG-PET uptakes in already-atrophic regions are not reliable for modeling the underlying neurodegeneration occurring in this scenario. Conversely, frontotemporal FDG-PET SUVR measures — and not cortical thinning or gray matter volume — would appropriately characterize disease progression in early-stage HD. This could have important implications in clinical trials using imaging biomarkers to evaluate increases in brain metabolism or neuroprotective effects in this population [21].

The strengths of this study include the use of a relatively large and representative sample of premanifest and early-stage HD patients, where the latter group showed an initial clinical decay in motor, cognitive, and neuropsychiatric indicators without a significant difference in genetic burden. Additionally, we applied for the first time a novel surface-based technique to study intracortical FDG-PET uptake changes in early HD. This work has several limitations. First, it is a cross-sectional study, which hinders interpretation of results with respect to a longitudinal approach. Secondly, it

Table 2 Comparison of subcortical volumes and mean FDG-PET PVC-SUVr values

Measure	Hemisphere	Subcortical region	PreHD	EarlyHD	Adjusted <i>P</i> -val
Volume (ml)	Left	Caudate	2.9 ± 0.4	2.1 ± 0.3	< 0.0001 ^{*a}
		Putamen	3.9 ± 0.7	2.9 ± 0.5	0.002 ^{*a}
		Accumbens	0.4 ± 0.09	0.3 ± 0.1	0.3
		Pallidum	1.7 ± 0.2	1.3 ± 0.3	< 0.0001 ^{*a}
		Amygdala	1.3 ± 0.2	1.2 ± 0.3	0.7
		Thalamus	7.3 ± 0.9	6.7 ± 0.7	0.3
		Hippocampus	3.8 ± 0.4	3.6 ± 0.5	0.8
	Right	Caudate	3.1 ± 0.4	2.3 ± 0.5	< 0.0001 ^{*a}
		Putamen	3.8 ± 0.7	2.8 ± 0.4	0.002 ^{*a}
		Accumbens	0.5 ± 0.08	0.4 ± 0.07	0.03 [*]
		Pallidum	1.7 ± 0.2	1.3 ± 0.2	< 0.0001 ^{*a}
		Amygdala	1.5 ± 0.2	1.4 ± 0.2	0.2
		Thalamus	6.6 ± 0.8	6.5 ± 0.7	0.6
		Hippocampus	3.9 ± 0.4	3.7 ± 0.4	0.6
FDG-PET PVC-SUVr	Left	Caudate	2.1 ± 0.3	1.2 ± 0.2	< 0.0001 ^{*a}
		Putamen	2.2 ± 0.3	1.4 ± 0.2	< 0.0001 ^{*a}
		Accumbens	1.7 ± 0.2	1.6 ± 0.4	0.2
		Pallidum	1.1 ± 0.1	1.0 ± 0.1	0.4
		Amygdala	1.1 ± 0.1	1.0 ± 0.1	0.2
		Thalamus	1.7 ± 0.2	1.7 ± 0.1	0.9
		Hippocampus	1.3 ± 0.1	1.2 ± 0.1	0.3
	Right	Caudate	2.0 ± 0.3	1.2 ± 0.2	< 0.0001 ^{*a}
		Putamen	2.2 ± 0.3	1.5 ± 0.2	< 0.0001 ^{*a}
		Accumbens	1.5 ± 0.2	1.4 ± 0.3	0.2
		Pallidum	1.2 ± 0.1	1.0 ± 0.1	0.1
		Amygdala	1.1 ± 0.1	1.1 ± 0.1	0.3
		Thalamus	1.7 ± 0.2	1.7 ± 0.1	0.8
		Hippocampus	1.3 ± 0.1	1.2 ± 0.1	0.2

Values are expressed as mean ± standard deviation. *P*-values are adjusted for age, sex, and education

^a Surviving false discovery rate (FDR) correction for multiple comparisons

**p* < 0.05

lacked advanced-stage HD and control groups. Nonetheless, we focused on the characterization of initial disease progression by comparing premanifest to early-HD patients, which has the highest potential to be studied in clinical trials [22]. In addition, describing deviations from normal brain structure and metabolism in HD patients, which was not our research objective, have already been reported [3, 23]. Besides, the massive cortical atrophy observed in advanced-stage HD patients [24] would probably imply a limited therapeutic potential and also diminish the value of FDG-PET imaging.

Overall, our findings reveal a differential metabolic and structural cortical degeneration in the transition from premanifest to early-stage HD that characterize the clinical worsening of these individuals. These results provide further evidence that early disease progression in HD individuals is not exclusively driven by a frontostriatal compromise, but

rather by a complex neurodegenerative process involving frontotemporal and parieto-occipital deterioration.

Acknowledgements The authors wish to thank all those at the Hospital de la Santa Creu i Sant Pau involved in the study. The authors also wish to thank the study participants and their families.

Funding This study was partially funded by a Spanish Government Grant (PI17/001885).

Compliance with ethical standards

Conflict of interest Author Frederic Sampedro declares that he has no conflict of interest. Author Saul Martínez-Horta declares that he has no conflict of interest. Author Jesus Perez-Perez declares that he has no conflict of interest. Author Andrea Horta-Barba declares that she has no conflict of interest. Author Diego-Alfonso Lopez-Mora declares that he has no conflict of interest. Author Valle Camacho declares that she has no

conflict of interest. Author Alejandro Fernandez-Leon declares that he has no conflict of interest. Author Beatriz Gomez-Anson declares that she has no conflict of interest. Author Ignasi Carrió declares that he has no conflict of interest. Author Jaime Kulisevsky declares that he has no conflict of interest.

Ethical approval All procedures performed in studies involving human participants were in accordance with the ethical standards of the institutional and/or national research committee and with the 1964 Helsinki Declaration and its later amendments or comparable ethical standards.

Informed consent Informed consent was obtained from all individual participants included in the study.

Publisher's Note Springer Nature remains neutral with regard to jurisdictional claims in published maps and institutional affiliations.

References

- Ross CA, Tabrizi SJ. Huntington's disease: from molecular pathogenesis to clinical treatment. *Lancet Neurol*. 2011;10:83–98.
- Nopoulos PC, Aylward EH, Ross CA, Johnson HJ, Magnotta VA, Juhl AR, et al. Cerebral cortex structure in prodromal Huntington disease. *Neurobiol Dis*. 2010;40:544–54.
- Scahill RI, Andre R, Tabrizi SJ, Aylward EH. Structural imaging in premanifest and manifest Huntington disease. *Handb Clin Neurol*. 2017;144:247–61.
- Tabrizi SJ, Langbehn DR, Leavitt BR, Roos RA, Durr A, Craufurd D, et al. Biological and clinical manifestations of Huntington's disease in the longitudinal TRACK-HD study: cross-sectional analysis of baseline data. *Lancet Neurol*. 2009;8:791–801.
- Iwamoto T, Utsumi K, Kobayashi S, Yasumura S, Hatakeyama S, Hayashi A, et al. Effect of memantine on brain metabolic activity and perfusion in drug-naïve moderate Alzheimer's disease patients. *Neuropsychiatry*. 2018;08:546–54.
- Small GW, Siddarth P, Silverman DHS, Ercoli LM, Miller KJ, Lavretsky H, et al. Cognitive and cerebral metabolic effects of celecoxib versus placebo in people with age-related memory loss: randomized controlled study. *Am J Geriatr Psychiatry*. 2008;16:999–1009.
- Hjermind LE, Law I, Jønch A, Stokholm J, Nielsen JE. Huntington's disease: effect of memantine on FDG-PET brain metabolism? *J Neuropsychiatr Clin Neurosci*. 2011;23:206–10.
- Pagano G, Niccolini F, Politis M. Current status of PET imaging in Huntington's disease. *Eur J Nucl Med Mol Imaging*. 2016;43:1171–82.
- Greve DN, Salat DH, Bowen SL, Izquierdo-Garcia D, Schultz AP, Catana C, et al. Different partial volume correction methods lead to different conclusions: an (18)F-FDG-PET study of aging. *NeuroImage*. 2016;132:334–43.
- Greve DN, Svarer C, Fisher PM, Feng L, Hansen AE, Baare W, et al. Cortical surface-based analysis reduces bias and variance in kinetic modeling of brain PET data. *NeuroImage*. 2014;92:225–36.
- Martinez-Horta S, Perez-Perez J, van Duijn E, Fernandez-Bobadilla R, Carceller M, Pagonabarraga J, et al. Neuropsychiatric symptoms are very common in premanifest and early stage Huntington's disease. *Parkinsonism Relat Disord*. 2016;25:58–64.
- Kingma EM, van Duijn E, Timman R, van der Mast RC, Roos RAC. Behavioural problems in Huntington's disease using the problem behaviours assessment. *Gen Hosp Psychiatry*. 2008;30:155–61.
- Martínez-Horta S, Perez-Perez J, Sampedro F, Pagonabarraga J, Horta-Barba A, Carceller-Sindreu M, et al. Structural and metabolic brain correlates of apathy in Huntington's disease. *Mov Disord*. 2018;33:1151–9.
- Varrone A, Asenbaum S, Vander Borght T, Booij J, Nobili F, Någren K, et al. EANM procedure guidelines for PET brain imaging using [18F]FDG, version 2. *Eur J Nucl Med Mol Imaging*. 2009;36:2103–10.
- Fischl B, Dale AM. Measuring the thickness of the human cerebral cortex from magnetic resonance images. *Proc Natl Acad Sci U S A*. 2000;97:11050–5.
- Lopez-Mora DA, et al. Selection of reference regions to model neurodegeneration in Huntington's disease by FDG-PET/CT using imaging and clinical parameters. *Clin Nucl Med*. 2018;44(1):e1–e5.
- Labuschagne I, Cassidy AM, Scahill RI, Johnson EB, Rees E, O'Regan A, et al. Visuospatial processing deficits linked to posterior brain regions in premanifest and early stage Huntington's disease. *J Int Neuropsychol Soc*. 2016;22:595–608.
- Johnson EB, Rees EM, Labuschagne I, Durr A, Leavitt BR, Roos RAC, et al. The impact of occipital lobe cortical thickness on cognitive task performance: an investigation in Huntington's disease. *Neuropsychologia*. 2015;79:138–46.
- Starkstein SE, Brandt J, Bylsma F, Peyser C, Folstein M, Folstein SE. Neuropsychological correlates of brain atrophy in Huntington's disease: a magnetic resonance imaging study. *Neuroradiology*. 1992;34:487–9.
- Coppen EM, van der Grond J, Hafkemeijer A, Barkey Wolf JJH, Roos RAC. Structural and functional changes of the visual cortex in early Huntington's disease. *Hum Brain Mapp*. 2018;39(12):4776–86.
- Arney K. Improved metrics for Huntington's disease trials. *Nature*. 2018;557:S46–7.
- Tabrizi SJ, Reilmann R, Roos RAC, Durr A, Leavitt B, Owen G, et al. Potential endpoints for clinical trials in premanifest and early Huntington's disease in the TRACK-HD study: analysis of 24 month observational data. *Lancet Neurol*. 2012;11:42–53.
- López-Mora DA, Camacho V, Pérez-Pérez J, Martínez-Horta S, Fernández A, Sampedro F, et al. Striatal hypometabolism in premanifest and manifest Huntington's disease patients. *Eur J Nucl Med Mol Imaging*. 2016;43:2183–9.
- Rosas HD, Liu AK, Hersch S, Glessner M, Ferrante RJ, Salat DH, et al. Regional and progressive thinning of the cortical ribbon in Huntington's disease. *Neurology*. 2002;58:695–701.